JPCL2013

DATASET · OCTOBER 2014

READS
30

2 AUTHORS:

Takanori Komatsu
Yokohama City University
7 PUBLICATIONS **28** CITATIONS
SEE PROFILE

Jun Kikuchi
RIKEN
152 PUBLICATIONS **3,124** CITATIONS
SEE PROFILE

THE JOURNAL OF PHYSICAL CHEMISTRY Letters

Letter

pubs.acs.org/JPCL

Selective Signal Detection in Solid-State NMR Using Rotor-Synchronized Dipolar Dephasing for the Analysis of Hemicellulose in Lignocellulosic Biomass

Takanori Komatsu[†,‡] and Jun Kikuchi*[,†,‡,§,∥]

[†]RIKEN Center for Sustainable Resource Science, 1-7-22 Suehiro-cho, Tsurumi-ku, Yokohama 235-0045, Japan

[‡]Graduate School of Medical Life Science, Yokohama City University, 1-7-29 Suehirocho, Tsurumi-ku, Yokohama 230-0045, Japan

[§]Biomass Engineering Research Program, RIKEN Research Cluster for Innovation, 2-1 Hirosawa, Wako 351-0198, Japan

[∥]Graduate School of Bioagricultural Sciences and School of Agricultural Sciences, Nagoya University, 1 Furo-cho, Chikusa-ku, Nagoya 464-8601, Japan

Supporting Information

ABSTRACT: Solid-state dipolar dephasing filtered (DDF)-INADEQUATE experiments were used to detect the hemicellulosic signals of lignocellulosic mixtures; here dipolar dephasing was used as a signal filter to remove signals derived from cellulose. The maximum filtering efficiency was obtained when the dephasing time was adjusted to half the rotor period at a magic-angle spinning (MAS) frequency of 12 kHz, which indicated that the molecular motions in hemicelluloses are faster than those in cellulose. In a DDF-INADEQUATE spectrum of uniformly ^{13}C-labeled lignocellulose from corn (*Zea mays*) collected with a dephasing time of $1/2\nu_{MAS}$, the chemical shifts of β-D-xylopyranose (Xyl*p*) and α-L-arabinofuranose (Ara*f*) in glucuronoarabinoxylan, the major hemicellulose in the secondary cell walls of the gramineous plant, were assigned.

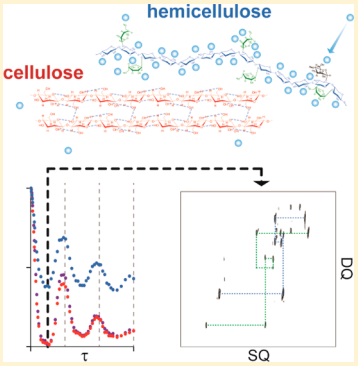

SECTION: Biophysical Chemistry and Biomolecules

NMR spectroscopy can provide insight into both the structure and dynamics of organic and inorganic molecules.[1−4] Solid-state NMR can be used to solve complex structures, even in complex heterogeneous multiphase environmental samples, including plant cell walls.[5−7] However, severe signal overlapping in the solid-state NMR spectra of complex samples limits the amount of information that can be obtained. Therefore, in this study, methods for the separation of signals in the solid-state NMR spectra of hemicellulose in a lignocellulosic biomass mixture were developed. The methods are based on the physicochemical properties of the components of the mixtures, which were analyzed using dipolar dephasing.

Lignocellulosic biomass has been identified as a carbon feedstock material with significant potential.[8] It is predominantly composed of cellulose, hemicellulose, and lignin. Unfortunately, our overall understanding of its supramolecular structure remains poor. Gel-state NMR techniques have been developed in conjunction with the use of pulverizing procedures and DMSO[9−12] or ionic liquid[13,14] solvent systems for the analysis of whole plant cell walls. Solid-state analysis techniques are desirable owing to their ability to reveal the supramolecular structure of lignocellulose, similar to the case where solid-state NMR was used to reveal the morphology of cellulose,[15−21] because the physical properties and highly ordered structures are expressed in the solid state.

Several problems are associated with the use of solid-state NMR, including the signal line width, which is typically broader than that obtained with solution NMR. Because of this the signals frequently overlap each other, especially in the region characteristic of polysaccharide signals (δ_{13C}: 60−110). In recent years, the investigation of the structural biology of proteins has become one of the most advanced applications of solid-state NMR. Optimization of sample preparation methods has led to significant improvement in spectral resolution, and this has consequently enabled the determination of the 3D structure of proteins using distance and orientation constraints.[22−24] However, with respect to lignocellulose, the signal resolution in the spectrum of the polysaccharides remains difficult even after sample optimizations have been performed because of the similarities in the polysaccharides' chemical shifts owing to their structural similarities. Moreover, although the heterogeneous molecular dynamics in polysaccharides provide important structural information, they can sometimes disrupt the signal analysis procedure. For example, in the cross-polarization (CP) experiment, signals derived from the rigid cellulose are more pronounced than those that correspond to

Received: May 11, 2013
Accepted: June 25, 2013

   dx.doi.org/10.1021/jz400978g | *J. Phys. Chem. Lett.* 2013, 4, 2279−2283

mobile hemicellulose, and the hemicellulosic signals therefore overlap the cellulosic signals.

Herein, we describe our attempt to optimize a method that provides a solution to the previously described problems related to the analysis of the hemicellulose in lignocellulose by solid-state NMR using a combination of simple signal filtering and multidimensional NMR. While relaxation time analyses provided information about the molecular dynamics of the polysaccharides in plant cell walls, the difference in the relaxation times was used for signal separation.[25,26] Spectral editing techniques based on relaxation time, chemical-shift anisotropy, and CP kinetics provide an alternative solution for signal separation.[27,28] In addition, spectral editing techniques have also been developed that divide signals on the basis of the number of attached protons.[29,30] Dipolar dephasing has traditionally been used for the selective detection of non-protonated carbon signals because the $^{1}H-^{13}C$ dipolar−dipolar interactions strongly facilitate the dissipation of the transverse magnetization in direct ^{1}H-bonded carbons.[31] However, sample hydration enabled hemicellulose to partially avoid the dissipation of the transverse magnetization because the molecular motions of the hemicellulose became faster after hydration.

Initially, we made several attempts to optimize the sample preparation process by hydration and introduce signal-filtering techniques using dipolar dephasing. CP-MAS spectra of the dried and hydrated uniformly ^{13}C-labeled lignocellulose from corn (*Zea mays*) (IsoLife, Wageningen, The Netherlands) are shown in Figure 1. Solid-state NMR spectra were recorded on

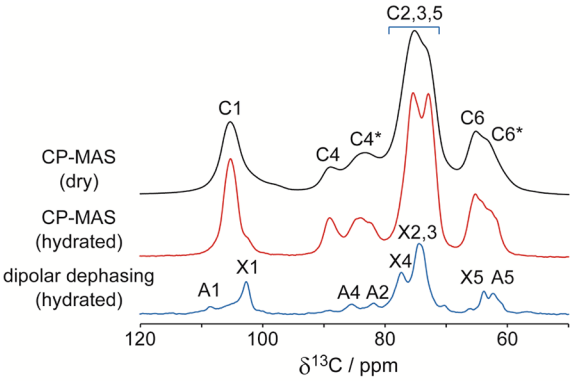

Figure 1. CP-MAS and dipolar dephasing spectra of dried and hydrated ^{13}C-labeled lignocellulose from corn. C represents the *β*-D-Glc*p* in cellulose and X and A represent the *β*-D-Xyl*p* and *β*-D-Ara*f* in glucuronoarabinoxylan, respectively.

an Avance-500 (Bruker, Billerica) spectrometer, equipped with a double-resonance 4-mm MAS probe; the instrument was operated at 500.132 MHz for the ^{1}H NMR spectra and 125.764 MHz for the ^{13}C NMR spectra. All of the NMR samples were maintained at a temperature of 298 K, and the magic-angle spinning (MAS) frequency was adjusted to 12 kHz. The hydration led to an increase in the rate of molecular motion, and subsequently, the line widths in the spectra of the hydrated samples became sharp. The dipolar dephasing spectrum of the hydrated sample is shown in Figure 1c. Signals that correspond to the *β*-D-Xyl*p* and *α*-L-Ara*f* in glucuronoarabinoxylan,[32] which is the major hemicellulose in the secondary cell walls of gramineous plants, remained unchanged, whereas the signals derived from the cellulose decayed. This change occurred because of the efficient hydration of the hemicellulose. In contrast, the cellulose, which exhibits hydrophobic properties because the hydrophilic planes of the glucopyranose are packed together through hydrogen-bonding interactions,[33] was poorly hydrated.

We then proceeded to investigate the filtering properties of the dipolar dephasing process as a function of the dephasing time. The relaxation curves from the $[\tau\text{-}180^{\circ}\text{-}\tau]$ dipolar dephasing experiment are shown in Figure 2. The chemical

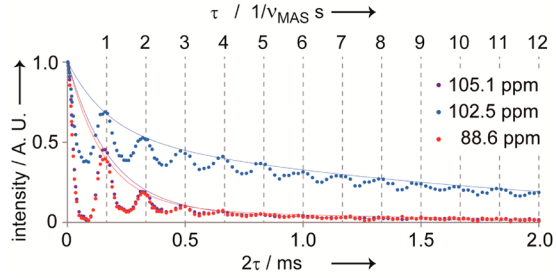

Figure 2. Relaxation curves for the dipolar dephasing experiments. The relaxation curves were modulated on the basis of the rotor period $(1/\nu_{MAS})$ because rotational echoes emerged. The relaxation curves are shown as solid lines. A double exponential function was used according to previous studies.[39,40].

shifts at 105.1, 102.5, and 88.6 ppm represent the signals from C1 of the I*β* crystal and the amorphous cellulose, C1 of the *β*-D-Xyl*p* in glucuronoarabinoxylan, and C4 of the I*β* crystal cellulose, respectively. The signal intensities at 105.1 and 88.6 ppm were diminished to almost zero until the dephasing time (τ) reached $1/2\nu_{MAS}$. The signals then reached approximately 40−50% of the initial value until the dephasing time reached $1/\nu_{MAS}$. The signal intensities subsequently reduced to zero when they were modulated with the rotor period $(1/\nu_{MAS})$. In this particular case, ν_{MAS} represents the MAS frequency. In contrast, the intensities of the signals at 102.5 ppm remained at approximately 40% of the initial value during the half rotor period $(1/2\nu_{MAS})$ and subsequently reduced gradually when modulated with the rotor period.

The relaxation curves were modulated by changes in the rotor period due to the rotational echoes that occurred because of the refocusing of the dephased transverse magnetization during the rotor period.[34,35] In one rotational period of dipolar dephasing experiments, signal intensities in the initial dephasing period exhibited a simple Gaussian decay; in contrast, at $\tau > 1/2\nu_{MAS}$, the signal intensities were dominated by rotational recoupling.[36] Therefore, the maximum efficiency for signal separation between the rigid and mobile components was obtained when the dephasing time was adjusted to half the rotor period at 12 kHz MAS frequency in the experiment.

Similar to dipolar dephasing experiments, DIPSHIFT is a type of separated local field spectroscopy used to determine the heteronuclear dipolar coupling strength that might be scaled down by fast molecular dynamics that occur with correlation times within the range of 10^{-5} to 10^{-4} s.[35,37−40] Therefore, the modulation behavior observed in this study indicated that glucuronoarabinoxylan molecules have molecular motion of 10^{-5} to 10^{-4} s. Relaxation curves fitted using only the intensities in the rotor period are shown in Figure 2 as solid lines, and the calculated values of the relaxation time constant are shown in Figure S2 in the Supporting Information. The *T2′* value of the signal at 102.5 ppm was also significantly greater than those of

dx.doi.org/10.1021/jz400978g | J. Phys. Chem. Lett. 2013, 4, 2279−2283

the signals at 105.1 and 88.6 ppm, which indicates that the molecular motions in glucuronoarabinoxylan were significantly faster than those in cellulose.

The DDF-INADEQUATE pulse sequence successively detected the hemicellulosic signals in lignocellulose by suppressing the cellulosic signals. As shown in Figure 3a, this pulse sequence was applied in the form of a variable-amplitude CP process, and a [τ-180°-τ] dipolar dephasing was then conducted. A *J*-INADEQUATE-type mixing and evolving process was then employed, and the free induced decay was recorded. The DDF-INADEQUATE spectra with dephasing times of $1/\nu_{MAS}$ and $1/2\nu_{MAS}$ are shown in Figure 3b,c, respectively. Analysis of the signals from the β-D-Xyl*p* and α-L-Ara*f* in the DDF-INADEQUATE spectrum with a dephasing time of $1/\nu_{MAS}$ remained difficult, with the exception of the C1 and C5 signals, because the strong rotational echoes of the cellulose overlapped with the β-D-Xyl*p* and α-L-Ara*f* signals. In contrast, in the DDF-INADEQUATE spectrum with a dephasing time of $1/2\nu_{MAS}$, the signals from the cellulose were completely suppressed and the signals from β-D-Xyl*p* and α-L-Ara*f* could be easily assigned. The ^{13}C chemical shifts of β-D-Xyl*p* and α-L-Ara*f* in glucuronoarabinoxylan were identified at 102.5 ($\delta_{C1\text{-}Xyl}$), 73.8 ($\delta_{C2\text{-}Xyl}$), 74.7 ($\delta_{C3\text{-}Xyl}$), 77.2 ($\delta_{C4\text{-}Xyl}$), 63.8 ($\delta_{C5\text{-}Xyl}$), 108.4 ($\delta_{C1\text{-}Ara}$), 81.7 ($\delta_{C2\text{-}Ara}$), 78.2 ($\delta_{C3\text{-}Ara}$), 85.8 ($\delta_{C4\text{-}Ara}$), and 62.3 ($\delta_{C5\text{-}Ara}$) ppm.

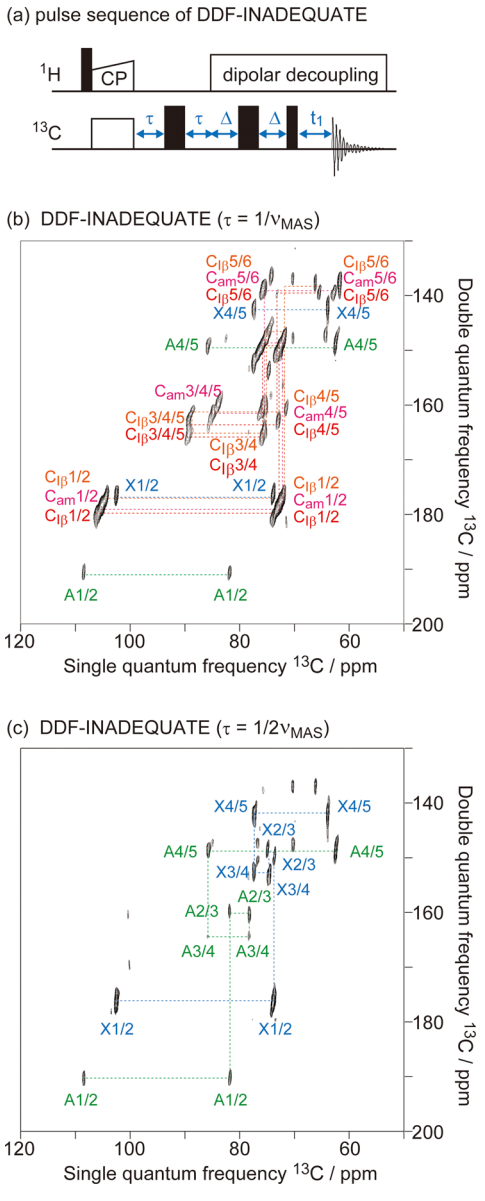

Figure 3. DDF-INADEQUATE pulse sequence successively detects and assigns hemicellulosic signals in lignocellulose. (a) Pulse sequence of the DDF-INADEQUATE experiment. (b) DDF-INADEQUATE spectra with a dephasing time of $1/\nu_{MAS}$. Partial rotational echoes of the cellulose prevented hemicellulosic signal assignment. (c) DDF-INADEQUATE spectra with a dephasing time of $1/2\nu_{MAS}$. The cellulosic signals were completely dephased during this period.

When the DDF-INADEQUATE experiment was conducted for the ^{13}C-labeled lignocellulose from potato, the signals of the α-D-Xyl*p* and α-L-Ara*f* in the arabinoxyloglucan,[42,43] the major hemicellulose in the primary cell walls of solanaceous plants, were effectively assigned (Figure S3 in the Supporting Information). The ^{13}C chemical shift of α-D-Xyl*p* and α-L-Ara*f* in arabinoxyloglucan were identified at 99.7 ($\delta_{C1\text{-}Xyl}$), 72.4 ($\delta_{C2\text{-}Xyl}$), 73.8 ($\delta_{C3\text{-}Xyl}$), 70.4 ($\delta_{C4\text{-}Xyl}$), 62.2 ($\delta_{C5\text{-}Xyl}$), 110.0 ($\delta_{C1\text{-}Ara}$), 82.0 ($\delta_{C2\text{-}Ara}$), 77.4 ($\delta_{C3\text{-}Ara}$), 84.8 ($\delta_{C4\text{-}Ara}$), and 62.2 ($\delta_{C5\text{-}Ara}$) ppm. The method introduced in this context effectively revealed structural differences in cell walls of plants from different plant families. In addition, distance-dependent mixing, such as radio frequency-driven recoupling (RFDR),[44] proton-driven spin diffusion (PDSD),[45] and dipolar assisted rotational resonance (DARR)[46] could be used for the DDF 2-D experiments by replacing the mixing with *J*-INADEQUATE (Figure 4). For example, pulse sequence and spectrum of DDF-DARR are shown in Figure 4a,b, respectively. These experiments will provide distance information for lignocellulose, whereas the measuring of the relaxation time will provide heterogeneous molecular dynamics of the polysaccharides. In conclusion, dipolar dephasing filtering 2D experiments represent a promising technique for revealing the supramolecular structure of lignocellulose.

MAS frequency plays an important role in dipolar dephasing experiments because rotational echoes emerge in rotor periods. In the dephasing period of the dipolar dephasing experiment, magnetization evolves under the influence of chemical shifts and dipolar−dipolar interactions. Although the influence of chemical shifts is removed by the 180° pulse, dipolar−dipolar interactions remain and result in the separation of signals according to their mobility. In the case of slow MAS, the adjustment of the dephasing time to half the rotor period is not necessarily the best choice because this period can also be too long for hemicelluloses to decay. Therefore, in general, the best filtering efficiency was obtained when the dephasing time was adjusted to the moment when the intensities of the filtering target signals approached zero. However, in the case of the very fast MAS, dipolar dephasing experiments are inefficient for signal separation because the dephasing time is insufficient when it is adjusted to half the rotor period. Therefore, techniques based on $T2'$ relaxation are more useful under such conditions.[36,41] $T2'$-relaxation-based filtering spectrum was obtained using the same pulse sequence used for the DDF-INADEQUATE experiments (where the dephasing time was n/ν_{MAS}), and the results are shown in Figure S4 in the Supporting Information. When the MAS frequency and dephasing time were adjusted to 12 kHz and 1 ms, respectively, this spectrum was similar to the DDF-INADEQUATE spectra with a dephasing time of $1/2\nu_{MAS}$.

dx.doi.org/10.1021/jz400978g | J. Phys. Chem. Lett. 2013, 4, 2279−2283

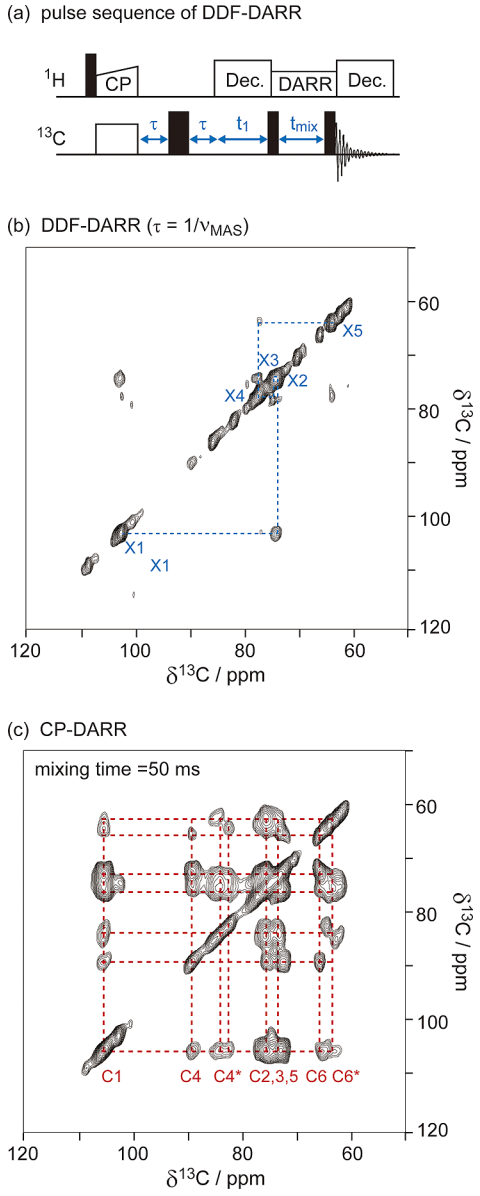

Figure 4. DDF-DARR spectra of hydrated ^{13}C-labeled lignocellulose from corn. (a) Pulse sequence of DDF-DARR. (b) DDF-DARR spectra of hydrated ^{13}C-labeled lignocellulose from corn with a mixing time of 50 ms ($\tau = 1/2\nu_{MAS}$). (c) CP-DARR spectra of the ^{13}C-labeled lignocellulose from corn with a mixing time (t_{mix}) of 50 ms. The ^{13}C−^{13}C correlation in α-L-Ara*f* was not detected under these conditions.

■ ASSOCIATED CONTENT

Ⓢ Supporting Information

Experimental details, the partial structures of glucuronoarabinoxylan and arabinoxyloglucan, CP-INADEQUATE spectra of dry and hydrated ^{13}C-labeled lignocellulose from corn, the DDF-INADEQUATE spectrum ^{13}C-labeled lignocellulose from potato analysis, a spectrum of *T2′*-edited INADEQUATE, a list of ^{13}C chemical shifts assigned in this study, and details of the relaxation analyses. This material is available free of charge via the Internet at http://pubs.acs.org.

■ AUTHOR INFORMATION

Corresponding Author

*E-mail: jun.kikuchi@riken.jp.

Notes

The authors declare no competing financial interests.

■ ACKNOWLEDGMENTS

The authors wish to thank Keiko Okushita (Yokohama City University) for help with the initial stage of this study. This research was partially supported by Grants-in-Aid for Scientific Research (C) (to J.K.) and Advanced Low Carbon Technology Research and Developmental Program (ALCA to J.K.), from Ministry of Education, Culture and Sports.

■ REFERENCES

(1) Andronesi, O. C.; Becker, S.; Seidel, K.; Heise, H.; Young, H. S.; Baldus, M. Determination of Membrane Protein Structure and Dynamics by Magic-Angle-Spinning Solid-State NMR Spectroscopy. *J. Am. Chem. Soc.* **2005**, *127*, 12965−12974.

(2) Asakura, T.; Ashida, J.; Yamane, T.; Kameda, T.; Nakazawa, Y.; Ohgo, K.; Komatsu, K. A Repeated Beta-Turn Structure In Poly(Ala-Gly) As A Model For Silk I Of Bombyx Mori Silk Fibroin Studied With Two-Dimensional Spin-Diffusion NMR Under Off Magic Angle Spinning And Rotational Echo Double Resonance. *J. Mol. Biol.* **2001**, *306*, 291−305.

(3) Ashbrook, S. E.; Whittle, K. R.; Lumpkin, G. R.; Farnan, I. Y-89 Magic-Angle Spinning NMR of $Y_2Ti_{2-x}Sn_xO_7$ Pyrochlores. *J. Phys. Chem. B* **2006**, *110*, 10358−10364.

(4) Deazevedo, E. R.; Saalwachter, K.; Pascui, O.; De Souza, A. A.; Bonagamba, T. J.; Reichert, D. Intermediate Motions as Studied by Solid-State Separated Local Field NMR Experiments. *J. Chem. Phys.* **2008**, 128.

(5) Simpson, A. J.; Simpson, M. J.; Soong, R. Nuclear Magnetic Resonance Spectroscopy and Its Key Role in Environmental Research. *Environ. Sci. Technol.* **2012**, *46*, 11488−11496.

(6) Bardet, M.; Foray, M. F.; Tran, Q. K. High-Resolution Solid-State CPMAS NMR Study of Archaeological Woods. *Anal. Chem.* **2002**, *74*, 4386−4390.

(7) Bardet, M.; Gerbaud, G.; Giffard, M.; Doan, C.; Hediger, S.; Le Pape, L. C-13 High-Resolution Solid-State NMR for Structural Elucidation of Archaeological Woods. *Prog. Nucl. Magn. Reson. Spectrosc.* **2009**, *55*, 199−214.

(8) Ragauskas, A. J.; Williams, C. K.; Davison, B. H.; Britovsek, G.; Cairney, J.; Eckert, C. A.; Frederick, W. J.; Hallett, J. P.; Leak, D. J.; Liotta, C. L.; et al. The Path Forward for Biofuels and Biomaterials. *Science* **2006**, *311*, 484−489.

(9) Mansfield, S. D.; Kim, H.; Lu, F. C.; Ralph, J. Whole Plant Cell Wall Characterization Using Solution-State 2D NMR. *Nat. Protoc.* **2012**, *7*, 1579−1589.

(10) Kim, H.; Ralph, J. Solution-State 2D NMR of Ball-Milled Plant Cell Wall Gels in DMSO-d(6)/Pyridine-d(5). *Org. Biomol. Chem.* **2010**, *8*, 576−591.

(11) Watanabe, T.; Shino, A.; Akashi, K.; Kikuchi, J. Spectroscopic Investigation of Tissue-Specific Biomass Profiling for *Jatropha Curcas* L. *Plant Biotechnol.* **2012**, *29*, 163−170.

(12) Ogata, Y.; Chikayama, E.; Morioka, Y.; Everroad, R. C.; Shino, A.; Matsushima, A.; Haruna, H.; Moriya, S.; Toyoda, T.; Kikuchi, J. ECOMICS: A Web-Based Toolkit for Investigating the Biomolecular Web in Ecosystems Using a Transomics Approach. *Plos One* **2012**, *7*.

(13) Cheng, K.; Sorek, H.; Zimmermann, H.; Wemmer, D. E.; Pauly, M. Solution-State 2D NMR Spectroscopy of Plant Cell Walls Enabled by a Dimethylsulfoxide-d6/1-Ethyl-3-methylimidazolium Acetate Solvent. *Anal. Chem.* **2013**, *85*, 3213−3221.

(14) Samuel, R.; Foston, M.; Jaing, N.; Cao, S. L.; Allison, L.; Studer, M.; Wyman, C.; Ragauskas, A. J. HSQC (Heteronuclear Single Quantum Coherence) C-13-H-1 Correlation Spectra of Whole Biomass in Perdeuterated Pyridinium Chloride-DMSO System: An Effective Tool for Evaluating Pretreatment. *Fuel* **2011**, *90*, 2836−2842.

(15) Atalla, R. H.; Vanderhart, D. L. Native Cellulose: A Composite of Two Distinct Crystalline Forms. *Science* **1984**, *223*, 283−285.

(16) Kono, H.; Erata, T.; Takai, M. Determination of the Through-Bond Carbon-Carbon and Carbon-Proton Connectivities of the Native Celluloses in the Solid State. *Macromolecules* **2003**, *36*, 5131−5138.
(17) Kono, H.; Yunoki, S.; Shikano, T.; Fujiwara, M.; Erata, T.; Takai, M. CP/MAS C-13 NMR Study of Cellulose and Cellulose Derivatives. 1. Complete Assignment of the CP/MAS C-13 NMR Spectrum of the Native Cellulose. *J. Am. Chem. Soc.* **2002**, *124*, 7506−7511.
(18) Cadars, S.; Lesage, A.; Emsley, L. Chemical Shift Correlations in Disordered Solids. *J. Am. Chem. Soc.* **2005**, *127*, 4466−4476.
(19) Mori, T.; Chikayama, E.; Tsuboi, Y.; Ishida, N.; Shisa, N.; Noritake, Y.; Moriya, S.; Kikuchi, J. Exploring the Conformational Space of Amorphous Cellulose Using NMR Chemical Shifts. *Carbohydr. Polym.* **2012**, *90*, 1197−1203.
(20) Witter, R.; Sternberg, U.; Hesse, S.; Kondo, T.; Koch, F. T.; Ulrich, A. S. C-13 Chemical Shift Constrained Crystal Structure Refinement of Cellulose I-alpha and Its Verification by NMR Anisotropy Experiments. *Macromolecules* **2006**, *39*, 6125−6132.
(21) Okushita, K.; Chikayama, E.; Kikuchi, J. Solubilization Mechanism and Characterization of the Structural Change of Bacterial Cellulose in Regenerated States Through Ionic Liquid Treatment. *Biomacromolecules* **2012**, *13*, 1323−1330.
(22) Castellani, F.; van Rossum, B.; Diehl, A.; Schubert, M.; Rehbein, K.; Oschkinat, H. Structure of a Protein Determined by Solid-State Magic-Angle-Spinning NMR Spectroscopy. *Nature* **2002**, *420*, 98−102.
(23) Martin, R. W.; Zilm, K. W. Preparation of Protein Nanocrystals and Their Characterization by Solid State NMR. *J. Magn. Reson.* **2003**, *165*, 162−174.
(24) Ketchem, R. R.; Hu, W.; Cross, T. A. High-Resolution Conformation of Gramicidin-a in a Lipid Bilayer by Solid-State NMR. *Science* **1993**, *261*, 1457−1460.
(25) Fenwick, K. M.; Apperley, D. C.; Cosgrove, D. J.; Jarvis, M. C. Polymer Mobility in Cell Walls of Cucumber Hypocotyls. *Phytochemistry* **1999**, *51*, 17−22.
(26) Tang, H. R.; Wang, Y. L.; Belton, P. S. C-13 CPMAS Studies of Plant Cell Wall Materials and Model Systems Using Proton Relaxation-Induced Spectral Editing Techniques. *Solid State Nucl. Mag.* **2000**, *15*, 239−248.
(27) Mao, J. D.; Holtman, K. M.; Franqui-Villanueva, D. Chemical Structures of Corn Stover and Its Residue after Dilute Acid Prehydrolysis and Enzymatic Hydrolysis: Insight into Factors Limiting Enzymatic Hydrolysis. *J. Agr. Food Chem.* **2010**, *58*, 11680−11687.
(28) Okushita, K.; Komatsu, T.; Chikayama, E.; Kikuchi, J. Statistical Approach for Solid-State NMR Spectra of Cellulose Derived From a Series of Variable Parameters. *Polym. J.* **2012**, *44*, 895−900.
(29) Mao, J. D.; Schmidt-Rohr, K. Methylene Spectral Editing in Solid-State C-13 NMR by Three-Spin Coherence Selection. *J. Magn. Reson.* **2005**, *176*, 1−6.
(30) Schmidt-Rohr, K.; Mao, J. D. Efficient Ch-Group Selection and Identification in C-13 Solid-State NMR by Dipolar Dept and H-1 Chemical-Shift Filtering. *J. Am. Chem. Soc.* **2002**, *124*, 13938−13948.
(31) Opella, S. J.; Frey, M. H. Selection of Non-Protonated Carbon Resonances in Solid-State Nuclear Magnetic Resonance. *J. Am. Chem. Soc.* **1979**, *101*, 5854−5856.
(32) Ebringerova, A.; Heinze, T. Xylan and Xylan Derivatives - Biopolymers With Valuable Properties, 1 - Naturally Occurring Xylans Structures, Procedures and Properties. *Macromol. Rapid Commun.* **2000**, *21*, 542−556.
(33) Nishiyama, Y.; Langan, P.; Chanzy, H. Crystal Structure and Hydrogen-Bonding System in Cellulose Ibeta from Synchrotron X-Ray and Neutron Fiber Diffraction. *J. Am. Chem. Soc.* **2002**, *124*, 9074−9082.
(34) Gullion, T.; Schaefer, J. Detection of Weak Heteronuclear Dipolar Coupling by Rotational-Echo Double-Resonance Nuclear Magnetic Resonance. *Adv. Magn. Opt. Reson.* **1989**, *13*, 57.
(35) Munowitz, M. G.; Griffin, R. G.; Bodenhausen, G.; Huang, T. H. Two-Dimensional Rotational Spin-Echo Nuclear Magnetic-Resonance in Solids - Correlation of Chemical-Shift and Dipolar Interactions. *J. Am. Chem. Soc.* **1981**, *103*, 2529−2533.
(36) Mao, K. M.; Kennedy, G. J.; Althaus, S. M.; Pruski, M. Spectral Editing in C-13 Solid-State NMR at High Magnetic Field Using Fast Mas and Spin-Echo Dephasing. *Solid State Nucl. Mag.* **2012**, *47−48*, 19−22.
(37) Hong, M.; Gross, J. D.; Griffin, R. G. Site-Resolved Determination of Peptide Torsion Angle Phi from the Relative Orientations of Backbone N-H and C-H Bonds by Solid-State NMR. *J. Phys. Chem. B* **1997**, *101*, 5869−5874.
(38) Hong, M.; Gross, J. D.; Rienstra, C. M.; Griffin, R. G.; Kumashiro, K. K.; Schmidt-Rohr, K. Coupling Amplification in 2D MAS NMR and Its Application to Torsion Angle Determination in Peptides. *J. Magn. Reson.* **1997**, *129*, 85−92.
(39) Dick-Perez, M.; Wang, T.; Salazar, A.; Zabotina, O. A.; Hong, M. Multidimensional Solid-State NMR Studies of the Structure and Dynamics of Pectic Polysaccharides in Uniformly C-13-Labeled Arabidopsis Primary Cell Walls. *Magn. Reson. Chem.* **2012**, *50*, 539−550.
(40) Dick-Perez, M.; Zhang, Y. A.; Hayes, J.; Salazar, A.; Zabotina, O. A.; Hong, M. Structure and Interactions of Plant Cell-Wall Polysaccharides by Two- and Three-Dimensional Magic-Angle-Spinning Solid-State NMR. *Biochemistry* **2011**, *50*, 989−1000.
(41) Mao, K. M.; Kennedy, G. J.; Althaus, S. M.; Pruski, M. Determination of the Average Aromatic Cluster Size of Fossil Fuels by Solid-State NMR at High Magnetic Field. *Energy Fuels* **2013**, *27*, 760−763.
(42) York, W. S.; Kolli, V. S. K.; Orlando, R.; Albersheim, P.; Darvill, A. G. The Structures of Arabinoxyloglucans Produced by Solanaceous Plants. *Carbohydr. Res.* **1996**, *285*, 99−128.
(43) Eda, S.; Kato, K. Studies on Chemical-Structure of Tobacco Hemicellulose 0.3. Arabinoxyloglucan Isolated from Midrib of Leaves of Nicotiana-Tabacum. *Agr. Biol. Chem.* **1978**, *42*, 351−357.
(44) Bennett, A. E.; Ok, J. H.; Griffin, R. G.; Vega, S. Chemical-Shift Correlation Spectroscopy in Rotating Solids - Radio Frequency-Driven Dipolar Recoupling and Longitudinal Exchange. *J. Chem. Phys.* **1992**, *96*, 8624−8627.
(45) Szeverenyi, N. M.; Sullivan, M. J.; Maciel, G. E. Observation of Spin Exchange by Two-Dimensional Fourier-Transform C-13 Cross Polarization-Magic-Angle Spinning. *J. Magn. Reson.* **1982**, *47*, 462−475.
(46) Takegoshi, K.; Nakamura, S.; Terao, T. C-13-H-1 Dipolar-Assisted Rotational Resonance in Magic-Angle Spinning NMR. *Chem. Phys. Lett.* **2001**, *344*, 631−637.